AIAA JOURNAL
Vol. 46, No. 1, January 2008

Technical Notes

TECHNICAL NOTES are short manuscripts describing new developments or important results of a preliminary nature. These Notes should not exceed 2500 words (where a figure or table counts as 200 words). Following informal review by the Editors, they may be published within a few months of the date of receipt. Style requirements are the same as for regular contributions (see inside back cover).

Thermodynamic Modeling of Hysteresis Effects in Piezoceramics for Application to Smart Structures

V. L. Sateesh,* C. S. Upadhyay,† and C. Venkatesan‡
Indian Institute of Technology, Kanpur 208 016, India

DOI: 10.2514/1.31885

Nomenclature

b_{kl}	=	electric susceptibility
C_{ijkl}	=	elastic constants
$\boldsymbol{E}$	=	electric field vector
E_C	=	coercive electric field
$E_{C\max}$	=	coercive electric filed corresponding to saturation polarization
e_{klm}	=	piezoelectric constants
H, Q	=	real constants
$\boldsymbol{P}$	=	polarization vector
P_r	=	remnant polarization
P_s	=	saturation polarization
$y_{i,M}$	=	deformation gradient tensor
α_{kl}	=	thermoelastic constants
$\beta_i, \xi, \Omega_{ij}, \zeta, \Gamma_i$	=	constants
ϵ_{ij}	=	strain
Θ	=	internal variable
θ	=	temperature difference
λ_k	=	pyroelectric constants
σ_{ij}	=	stress tensor
Ψ	=	Helmholtz free energy per unit volume

I. Introduction

WITH the development of piezoceramic sensors and actuators of varying shapes and sizes for use in structural applications, the field of smart structures has emerged as an area of research of great importance [1]. The mechanical, thermal, and electrical behavior of piezoceramics has been studied extensively by physicists and material scientists [2–9]. The introduction of these materials in structural applications has created a necessity to review the traditional structural modeling and analysis.

Presented as Paper 1743 at the 15-th AIAA/ASME/AHS Adaptive Structures Conference, Honolulu, HI, 23–26 April 2007; received 1 May 2007; accepted for publication 25 August 2007.

*Graduate Student, Department of Aerospace Engineering. Student Member AIAA.
†Associate Professor, Department of Aerospace Engineering.
‡Pandit Ramachandra Dwivedi Chair Professor, Department of Aerospace Engineering. Senior Member AIAA.

Under cyclic variation of the applied electric field, piezomaterials exhibit polarization-electric (P-E) field hysteretic losses, as shown in Fig. 1. The points indicated by the symbols P_s, P_r, and E_C represent saturation polarization, remnant polarization, and the coercive electric field, respectively. The saturation polarization P_s corresponds to the value of maximum polarization, which shows negligible change with further increase in electric field. Remnant polarization P_r is the value of polarization when the electric field becomes zero. Coercive electric field E_C corresponds to the points of zero polarization. The observed phenomenon is due to the delay in polarization switching with variation in electric field. P-E hysteresis effect leads to an interesting variation of strain with respect to electric field ($\epsilon - E$), and it is denoted as butterfly loop. The hysteresis will be affected by various parameters such as temperature, amplitude of oscillating electric field, frequency of oscillation, and external mechanical preloading. The effect of the amplitude of the electric field on the hysteresis loop has been studied experimentally by Nalwa [2]. It is observed that the remnant polarization and coercive electric field are functions of amplitude of the electric field. With a decrease in amplitude of the electric field, there is a reduction in the values of maximum polarization, remnant polarization, and coercive electric field. Viehland and Chen [3] experimentally studied the effects of frequency of oscillation of the electric field on the hysteresis loop. From the experiments, it was observed that if the amplitude of the electric field is above the coercive electric field $E_{C\max}$ corresponding to the case with saturation polarization, then the dissipation energy increases with an increase in frequency, whereas if the amplitude of the electric field is below $E_{C\max}$, then the dissipation energy increases with a decrease in frequency. The effect of mechanical preloading on hysteresis has been studied experimentally by Arndt et al. [4]. It is observed that when a compressive mechanical preloading is applied parallel to the electric field, the reduction in polarization is found to be higher than that corresponding to the case with mechanical loading applied perpendicular to the electrical field. With the application of compressive mechanical preloading, the remnant polarization and coercive field show a reduction in magnitude.

Mathematical modeling of hysteresis was approached at two different levels: 1) at the microscopic level and 2) at the macroscopic level of the piezomaterial. The microscopic models of hysteresis can be categorized as 1) polarization switching based on the Eshelby inclusion model [10], 2) crystal-plasticity-based nonlinear switching models [11], 3) free-energy-based domain-switching model [12], and 4) dipole–dipole interaction models with threshold-switching energy given by the time-dependent Ginzburg–Landau model [13,14] or the Landau–Devonshire model [15,16].

Macroscopic models can be categorized as either empirical models or thermodynamically consistent models. Empirical models are based on either introducing an additional variable in the constitutive relations [17], by representing the P-E curve by a tan-hyperbolic function [18], or by using the Presaich model [19,20]. Bassiouny et al. [21–24] developed a thermodynamic phenomenological model for capturing the electromechanical hysteresis effects based on the work-hardening plasticity model. A similar approach was followed by McMeeking and Landis [25] in modeling domain switching in ferroelectric materials. A model based on extended irreversible thermodynamics was proposed by Lu and Hanagud [26].

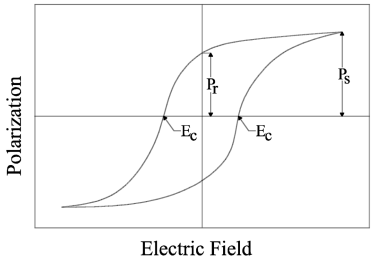

Fig. 1 P-E hysteresis loop for piezoelectric materials.

P-E hysteresis effects and the associated strain variations are macroscopic manifestations of irreversible microlevel variations in the crystal structure. By the method of local state [27,28], an internal variable can be introduced at the macroscopic level to represent the microlevel phenomenon. The method of local state postulates that the thermodynamic state of a material medium at a given point is completely defined by the knowledge of the values of a certain number of variables at that instant. A physical phenomenon can be described with precision depending on the choice of the number of state variables and their relation with the associated variables. The physical processes described in this manner will always be thermodynamically admissible provided Clausius–Duhem inequality is satisfied at every instant of evolution.

Even though micromechanical models have been able to capture hysteresis and butterfly loops, they are computationally time-consuming and cumbersome, particularly with regard to their application for structural analysis. Therefore, it is necessary to develop a thermodynamically consistent model that can be easily integrated with traditional finite element formulation for the analysis of smart structures. The objectives of this study are as follows:

1) Extend the electrothermoelastic formulation developed by the authors [29] to model the polarization-electric field hysteresis effects by a consistent thermodynamic formulation.

2) Validate the nonlinear constitutive model by comparing the theoretical and experimental hysteresis and butterfly-loop effects.

3) Study the variation of hysteresis loops with respective to the frequency of the electric field for the cases when the amplitude of the electric field is above and below the $E_{C\max}$.

4) Study the effects of variation in mechanical load and electric field on the hysteresis loops.

II. Thermodynamic Formulation

The mathematical formulation is based on continuum mechanics, electrostatics, and thermodynamic principles. The governing equations were developed by applying the conservation laws (mass, linear momentum, and angular momentum). The conservation of energy (first law of thermodynamics) and the rate of entropy production (second law of thermodynamics) are used for deriving the constitutive relations for piezomaterials. The development of the mathematical modeling of electrothermoelasticity follows the procedure given in [9,29,30]. The essential contribution of this paper is the development of a mathematical model to include the effects of electrical dissipation.

Using the method of local state, the free energy can be expressed as a function of state variables as

$$\Psi = \Psi(y_{j,M}, E_i, \Theta, \theta) \tag{1}$$

where $y_{j,M}$ is the deformation gradient tensor, E_i is electric field, θ is the temperature, and Θ is an internal variable representing the micromechanical phenomenon related to domain switching.

In the present formulation, the free energy Ψ is expressed as a quadratic function of all state variables and quartic functions of Green's strain and electric field.

$$\begin{aligned}\Psi = \tfrac{1}{2}[\{&C_{ijkl}\epsilon_{ij}\epsilon_{kl} - b_{ij}E_iE_j + C_\theta\theta^2 + \xi\Theta^2 - 2e_{ijk}E_i\epsilon_{jk} \\ &+ 2\alpha_{ij}\epsilon_{ij}\theta + 2\lambda_iE_i\theta - 2\Omega_{ij}\epsilon_{ij}\Theta - 2\beta_iE_i\Theta + 2\zeta\Theta\theta \\ &- Q_{ijkl}E_iE_jE_kE_l - H_{ijklm}\epsilon_{ij}E_kE_lE_m + f_{ijklmn}\epsilon_{ij}\epsilon_{kl}E_mE_n \\ &- g_{ijklmno}\epsilon_{ij}\epsilon_{kl}\epsilon_{mn}E_o + X_{ijklmnop}\epsilon_{ij}\epsilon_{kl}\epsilon_{mn}\epsilon_{op}\}\end{aligned} \tag{2}$$

Using Ψ, the set of constitutive relations between associated variables (force terms) and the state variables can be obtained. The evolution equation for internal variable is obtained by satisfying the inequality constraint on the energy dissipation. The final set of electrothermoelastic constitutive relations, including electric hysteresis effects, are given as

$$\begin{aligned}\sigma_{ij} = &C_{ijkl}\epsilon_{kl} - e_{ijk}E_k - H_{ijklm}E_kE_lE_m - \alpha_{ij}\theta - \Omega_{ij}\Theta - P_iE_j \\ &+ f_{ijklmn}\epsilon_{kl}E_mE_n - g_{ijklmno}\epsilon_{kl}\epsilon_{mn}E_o + X_{ijklmnop}\epsilon_{kl}\epsilon_{mn}\epsilon_{op}\end{aligned} \tag{3}$$

$$\begin{aligned}P_i = &b_{ij}E_j + Q_{ijkl}E_iE_jE_k + e_{ijk}\epsilon_{jk} + H_{ijklm}\epsilon_{jk}E_lE_m \\ &+ \beta_i\Theta - \lambda_i\theta - f_{ijklmn}\epsilon_{jk}\epsilon_{lm}E_n + g_{ijklmno}\epsilon_{jk}\epsilon_{lm}\epsilon_{no}\end{aligned} \tag{4}$$

$$S = \alpha_{ij}\epsilon_{ij} + \lambda_kE_k + C_\theta\theta - \zeta\Theta \tag{5}$$

$$\dot{\Theta} = -\left[\sum_{i=1,3,5\ldots}\left(\Gamma_i\frac{\partial\Psi}{\partial\Theta}\right)^i + \sum_{j=2,4,6\ldots}\Gamma_j\left(\Gamma_j\frac{\partial\Psi}{\partial\Theta}\right)^{j-1}\left|\frac{\partial\Psi}{\partial\Theta}\right|\right] \tag{6}$$

where

$$\frac{\partial\Psi}{\partial\Theta} = \xi\Theta - \beta_iE_i - \Omega_{ij}\epsilon_{ij} + \zeta\theta \tag{7}$$

C_{ijkl} is the elastic constant; b_{kl} is the electric susceptibility; C_θ is the thermal constant; e_{ijl} is the piezoelectric constant; α_{ij} is the thermoelastic constant; λ_i is the pyroelectric constant; ξ, β_i, Ω_{ij}, ζ, and Γ_i are real positive constants; and H_{ijklm} are Q_{ijkl} real constants. The mathematical details of this formulation can be found in [31].

III. Results and Discussion

Using the nonlinear constitutive relations given in Eqs. (3–7), the effects of frequency, amplitude of the electric field, and mechanical preload were studied. The mathematical model is validated by comparing the theoretical results with the experimental data on hysteresis effects available in the literature. The results are generated with and without mechanical loading and these are presented in the following sections.

A. Without Mechanical Preloading

The validity of the constitutive relations given in Eqs. (3–7) are verified by solving the problem of the free piezopatch subjected to an external time-varying electric field along the z direction. Neglecting temperature effects, the nonlinear electroelastic constitutive relations applicable for a 1D problem can be written as

$$\begin{aligned}\sigma_{33} = &C_{3333}\epsilon_{33} - e_{333}E_3 - H_{33333}E_3E_3E_3 - \Omega_{33}\Theta - P_3E_3 \\ &+ f_{333333}\epsilon_{33}E_3E_3 - g_{3333333}\epsilon_{33}\epsilon_{33}E_3 + X_{33333333}\epsilon_{33}\epsilon_{33}\epsilon_{33}\end{aligned} \tag{8}$$

$$\begin{aligned}P_3 = &b_{33}E_3 + Q_{3333}E_3E_3E_3 + e_{333}\epsilon_{33} + H_{33333}\epsilon_{33}E_3E_3 \\ &+ \beta_3\Theta - f_{333333}\epsilon_{33}\epsilon_{33}E_3 + g_{3333333}\epsilon_{33}\epsilon_{33}\epsilon_{33}\end{aligned} \tag{9}$$

$$\dot{\Theta} = -\left[\sum_{i=1,3,5\ldots}\left(\Gamma_i\frac{\partial\Psi}{\partial\Theta}\right)^i + \sum_{j=2,4,6\ldots}\Gamma_j\left(\Gamma_j\frac{\partial\Psi}{\partial\Theta}\right)^{j-1}\left|\frac{\partial\Psi}{\partial\Theta}\right|\right] \tag{10}$$

where

$$\frac{\partial \Psi}{\partial \Theta} = \xi\Theta - \beta_3 E_3 - \Omega_{33}\epsilon_{33} \tag{11}$$

because the piezopatch is treated as a free crystal, $\sigma_3 = 0$. Hence, from Eq. (8), strain in the z direction can be written as

$$\epsilon_{33} = \frac{[e_{333}E_3 + H_{33333}E_3E_3E_3 + \Omega_{33}\Theta + E_3P_3]}{C_{3333} + f_{333333}E_3E_3} + \underline{\frac{g_{3333333}\epsilon_{33}\epsilon_{33}E_3 - X_{33333333}\epsilon_{33}\epsilon_{33}\epsilon_{33}}{C_{3333} + f_{333333}E_3E_3}} \tag{12}$$

The underlined term represents the nonlinear effects in strain. The values of all the material constants used in the constitutive models are as follows:

1) The materials properties of PZT are $C_{33} = 117$ GPa, $e_{3333} = 23.3\ \mathrm{C\,m^{-2}}$, and $b_{33} = 1.30095\text{E-}8\ \mathrm{C^2\,N^{-1}\,m^{-2}}$.

2) Constants in the internal variable equation are $\xi = 0.00106$ GPa, $\Omega_{33} = 0.323$ GPa, $\beta_3 = 0.2594\ \mathrm{C\,m^{-2}}$, $H_{33333} = -5.2\text{E-}12$, $Q_{3333} = -7\text{E-}20$, $f_{333333} = 0$, $g_{3333333} = 0$, and $X_{33333333} = 0$.

3) The values of Γ $(\mathrm{m\,N^{-1}\,s^{-1}})$ are $\Gamma_1 = 2.26\text{E-}11$, $\Gamma_2 = 3.16\text{E-}10$, $\Gamma_3 = 13.2\text{E-}8$, $\Gamma_4 = 11.0\text{E-}8$, $\Gamma_5 = 2.72\text{E-}7$, $\Gamma_6 = 4.47\text{E-}07$, and $\Gamma_7 = 3.6106\text{E-}06$.

The material used is lead zirconate titanate (PZT), for which the constants corresponding to the linear part of model are taken from the literature. The coefficients of the nonlinear and dissipative terms were estimated based on error minimization between experimental and theoretical P-E hysteresis loop and also by imposing the limiting conditions on maximum polarization $P_{\max}$, maximum electric field $E_{\max}$, and maximum strain $\epsilon_{\max}$.

Assume that the piezopatch is acted on by an electric field having an amplitude of 2 kV/mm and a frequency of 0.0165 Hz. Keeping the initial conditions $P = 0$, $\epsilon = 0$, and $\Theta = 0$ at $t = 0$, the coupled nonlinear electroelastic Eqs. (9–12) are solved iteratively. The P-E hysteresis loop and the corresponding $\epsilon - E$ variation are shown in Figs. 2 and 3, respectively. These results are generated by keeping terms up to the seventh power in Eq. (10). It can be seen from Fig. 2 that the theoretically generated hysteresis loop correlates well with the experimental data [32], including both the initial variation and steady-state response. Figure 3 shows the corresponding variation of strain with respect to electric field (butterfly loop), and the correlation is satisfactory.

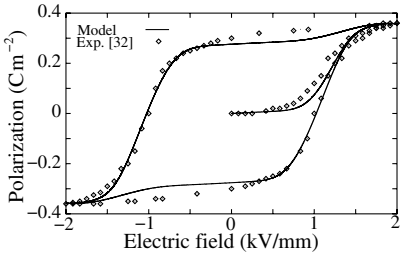

Fig. 2 Comparison of theoretical and experimental hysteresis loop.

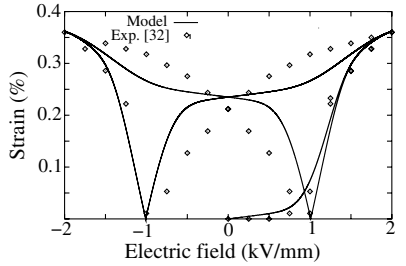

Fig. 3 Variation of strain with electric field (butterfly loop).

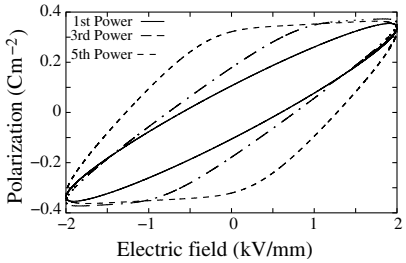

Fig. 4 Nature of hysteresis loops with an increasing order of nonlinearity.

For the sake of understanding, the influence of the order of the nonlinearity in Eq. (10) on the P-E hysteresis loop is analyzed. Figure 4 shows the variation in the hysteresis loops generated with different orders of nonlinearity. It can be seen that as the order of nonlinearity increases, the hysteresis loop tends to change from an ellipse to a rhombus shape.

To study the effect of amplitude of the electric field on hysteresis, hysteresis loops were generated for various amplitudes of the electric field, keeping all the other parameters and frequency (0.0165) as constants. With an increase in amplitude of the electric field, there is an increase in the size of hysteresis, as shown in Fig. 5, indicating an increase in energy loss. The remnant polarization and coercive electric fields are found to be functions of amplitude of the electric field. With a decrease in amplitude of the electric field, remnant polarization and the coercive electric field show a reduction. These observations are found to be in agreement with the experimental data given in Nalwa [2].

The influence of the frequency of oscillation of the electric field on the nature of the P-E hysteresis loop is also studied. Keeping the amplitude of the electric field as 2 kV/mm [which is above $E_{C\max}$ (i.e., 1 kV/mm from Fig. 3)], hysteresis loops were generated for three different frequencies of oscillating electric field: namely, 0.1, 1, and 10 Hz. It can be seen from Fig. 6 that increasing the frequency of oscillation of the electric field results in an increase in the area under the hysteresis loop, indicating increased energy loss. Figure 7 shows that when the amplitude of the electric field is 0.8 kV/mm (which is less than $E_{C\max}$), the dissipation energy increases with a decrease in the frequency. It is observed that when the amplitude of the electric field is above $E_{C\max}$, the magnitude of the coercive electric field increases with respect to increase in the frequency of oscillation of the electric field. When the amplitude of the electric field is below

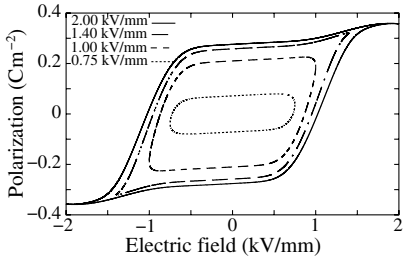

Fig. 5 Hysteresis loop for different amplitudes of the electric field.

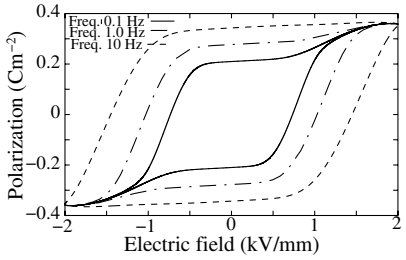

Fig. 6 Hysteresis loop for different frequencies of the electric field $E > E_{C\max}$.

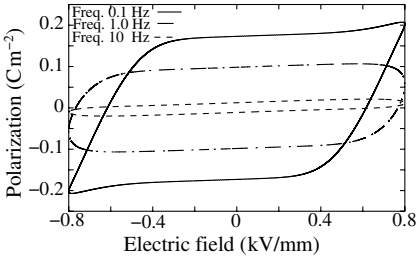

Fig. 7 Hysteresis loop for different frequencies of the electric field $E < E_{C\max}$.

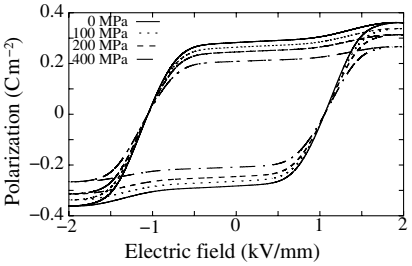

Fig. 9 Hysteresis loop with external mechanical preloading.

$E_{C\max}$, with an increase in frequency of the electric field, the magnitude of remnant polarization decreases. These observations are consistent with the experimental data given by Viehland and Chen [3].

B. Compressive Premechanical Loading

The effect of mechanical preloading on the hysteresis loop has been studied. In this case, the total strain consists of two parts: one part is due to the mechanical preloading and other part is caused by the time-varying electric field. The total strain can be written from Eq. (8) as

$$\epsilon_{33} = \frac{\sigma_{33}}{C_{3333} + f_{333333}E_3E_3} + \frac{[e_{333}E_3 + H_{33333}E_3E_3E_3 + \Omega_{33}\Theta + E_3P_3]}{C_{3333} + f_{333333}E_3E_3} + \frac{g_{3333333}\epsilon_{33}\epsilon_{33}E_3 - X_{33333333}\epsilon_{33}\epsilon_{33}\epsilon_{33}}{C_{3333} + f_{333333}E_3E_3} \tag{13}$$

The strain induced by the mechanical preloading is independent of time; that is, it will not evolve with the time. Hence, it is not required to include this component of strain in the internal variable evolution process [Eq. (11)]. Whereas, the strain induced by the time-varying electric field is rate-dependent and hence it alone should be considered in the internal variable evolution process. However, in the evaluation of polarization, the total strain given in Eq. (13) has to be substituted in Eq. (9). The total polarization can be written as

$$P_3 = P_e + P_m \tag{14}$$

where P_e represents the time-varying part of polarization, and P_m represents the component due to constant applied mechanical load. It is known that the effect of the compressive load is to reduce the magnitude of the polarization. Therefore, the sign of P_m has to be changed when the polarization P_e changes its direction. Using Eq. (14), the variation of total polarization P_3 with the electric field in the presence of compressive mechanical load (100 MPa) is evaluated and the variation is shown in Fig. 8a. From the figure, it can be seen that there is a jump in the curve when the polarization is changing its direction, because the sign of P_m has to be changed. It is known that the mechanical load cannot induce a polarization when the dipoles are randomly oriented (i.e., at points close to coercive electric field E_C). Therefore, a nondimensional parameter P_e/P_s is multiplied with the polarization term due to constant mechanical loading. The modified expression for total polarization can be written as

$$P_3 = P_e + \left(\frac{P_e}{P_s}\right)P_m \tag{15}$$

where P_s represents the saturation polarization for a free crystal. In this case, it is not necessary to change the sign of P_m, because the multiplication factor P_e/P_s takes care of the sign change. Using Eq. (15), the variation of polarization with electric field is evaluated and is shown in Fig. 8b. It can be seen that there is no discontinuity in the curve at E_C.

For various values of compressive preloading (applied parallel to the electric field), hysteresis loops were generated with Eq. (15), and they are shown in Fig. 9. It is observed from Fig. 9 that the area of the P-E hysteresis loop decreases with an increasing compressive preload. As the preloading increases, the remnant polarization shows a reduction in magnitude, as observed in experimental data presented in [4].

IV. Conclusions

In this study, a set of nonlinear electrothermoelastic constitutive relations was derived to model the electric hysteresis effects in a piezomaterial by following a consistent thermodynamic formulation. The nonlinear constitutive relations are shown to model the experimentally observed hysteresis and butterfly loops with reasonable accuracy.

The influence of amplitude and frequency of oscillation of the electric field on the hysteresis loop were analyzed. It is found that increasing the amplitude of the electric field increases the size of the hysteresis loop, indicating an increase in energy loss. If the amplitude of the electric field is above $E_{C\max}$, then the P-E hysteresis loss increases with an increase in frequency, whereas if the amplitude of the electric field is below $E_{C\max}$, then the dissipation energy decreases with an increase in frequency. These trends are observed to be consistent with the experimental observations available in the literature.

It is envisaged that the nonlinear electrothermoelastic formulation developed in this study can be easily integrated in the structural dynamic analysis of smart structures with embedded piezoactuators and sensors.

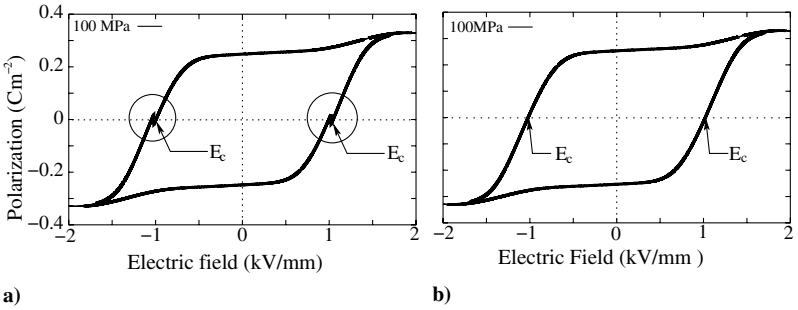

Fig. 8 Hysteresis loop with external mechanical preloading: a) using Eq. (14) and b) using Eq. (15).

References

[1] Crawley, E. F., "Intelligent Structures for Aerospace: A Technological Overview and Assessment," *AIAA Journal*, Vol. 31, No. 8, 1994, pp. 1689–1699.

[2] Nalwa, H. S., *Handbook of Low and High Dielectric Constant Materials and Their Applications*, Vol. 2, Academic Press, New York, 1999, pp. 113–136.

[3] Viehland, D., and Chen, Y -H., "Random-Field Model for Ferroelectric Domain Dynamics and Polarization Reversal," *Journal of Applied Physics*, Vol. 88, No. 11, 2000, pp. 6696–6707. doi:10.1063/1.1325001

[4] Arndt, H., Schmidt, G., and Vogel, N., "Influence of Uniaxial Pressure on the Properties of PLZT Ceramics," *Ferroelectrics*, Vol. 61, 1984, pp. 9–18. doi:10.1080/00150198408018931

[5] Cady, W. G., *Piezoelectricity Volumes I and II*, Dover, New York, 1946.

[6] Anderson, J. C., *Dielectrics*, Chapman and Hall, Boca Raton, FL, 1964, pp. 121–124.

[7] Jordan, T. L., and Ounaies, Z., "Piezoelectric Ceramics Characterization," NASA CR-211225, 2001.

[8] Toupin, R. A., "A Dynamical Theory of Elastic Dielectrics," *International Journal of Engineering Science*, Vol. 1, 1963, pp. 101–126. doi:10.1016/0020-7225(63)90027-2

[9] Tiersten, H. F., "On the Nonlinear Equations of Thermo-Electro-Elasticity," *International Journal of Engineering Science*, Vol. 9, 1971, pp. 587–604. doi:10.1016/0020-7225(71)90062-0

[10] Hwang, S. C., Huber, J. E., McMeeking, R. M., and Fleck, N. A., "The Simulation of Switching in Polycrystalline Ferroelectric Ceramics," *Journal of Applied Physics*, Vol. 84, No. 3, 1998, pp. 1530–1540. doi:10.1063/1.368219

[11] Huber, J. E., Fleck, N. A., Landis, C. M., and McMeeking, R. M., "A Constitutive Model for Ferroelectric Polycrystals," *Journal of the Mechanics and Physics of Solids*, Vol. 47, No. 8, 1999, pp. 1663–1697. doi:10.1016/S0022-5096(98)00122-7

[12] Shaikh, M. G., Phanish, S., and Sivakumar, S. M., "Domain Switching Criteria for Ferroelectrics," *Computational Materials Science*, Vol. 37, Nos. 1–2, 2006, pp. 178–186. doi:10.1016/j.commatsci.2005.12.040

[13] Hu, H. L., and Chen, L. Q., "Three-Dimensional Computer Simulation of Ferroelectric Domain Formation," *Journal of the American Ceramic Society*, Vol. 81, No. 3, 1998, pp. 492–500.

[14] Wang, J., Shi, S. Q., Chen, L. Q., Li, Y., and Zhang, T. Y., "Phase-Field Simulations of Ferroelectric/Ferroelastic Polarization Switching," *Acta Materialia*, Vol. 52, No. 3, 2004, pp. 749–764. doi:10.1016/j.actamat.2003.10.011

[15] Zhang, W., and Bhattacharya, K., "A Computational Model of Ferroelectric Domains, Part 1: Model Formulation and Domain Switching," *Acta Materialia*, Vol. 53, No. 1, 2005, pp. 185–198. doi:10.1016/j.actamat.2004.09.016

[16] Shu, Y. C., and Bhattacharya, K., "Domain Patterns and Macroscopic Behaviour of Ferroelectric Materials," *Philosophical Magazine*, Vol. 81, No. 12, 2001, pp. 2021–2054.

[17] Chen, P. J., and Montgomery, S. T., "A Macroscopic Theory for the Existence of the Hysteresis and Butterfly Loops in Ferroelectricity," *Ferroelectrics*, Vol. 23, 1980, pp. 199–208.

[18] Zhang, X. D., and Rogers, C. A., "A Macroscopic Phenomenological Formulation for Coupled Electromechanical Effects in Piezoelectricity," *Journal of Intelligent Material Systems and Structures*, Vol. 4, No. 3, 1993, pp. 307–316. doi:10.1177/1045389X9300400303

[19] Hughes, D., and Wen, J. T., "Preisach Modeling of Piezoceramic and Shape Memory Alloy Hysteresis," *Smart Materials and Structures*, Vol. 6, No. 3, 1997, pp. 287–300. doi:10.1088/0964-1726/6/3/007

[20] Bossong, H., Lentzen, S., and Schmidt, R., "Experimental Investigation and Modeling of Piezoelectric Actuator Hysteresis for FE Analysis of Smart Structures," Indo-German Discussion Meeting on Smart Materials and Structures, Indian Inst. of Technology, Dept. of Aerospace Engineering, Paper 9, 2005.

[21] Bassiouny, E., Ghaled, A. F., and Maugin, G. A., "Thermodynamical Formulation for Coupled Electromechanical Hysteresis Effects, 1: Basic Equations," *International Journal of Engineering Science*, Vol. 26, No. 12, 1988, pp. 1279–1295. doi:10.1016/0020-7225(88)90047-X

[22] Bassiouny, E., Ghaled, A. F., and Maugin, G. A., "Thermodynamical Formulation for Coupled Electromechanical Hysteresis Effects, 2: Poling of Ceramics," *International Journal of Engineering Science*, Vol. 26, No. 12, 1988, pp. 1297–1306.

[23] Bassiouny, E., Ghaleb, A. F., and Maugin, G. A., "Thermodynamical Formulation for Coupled Electromechanical Hysteresis Effects, 3: Parameter Identification," *International Journal of Engineering Science*, Vol. 27, No. 8, 1989, pp. 975–987. doi:10.1016/0020-7225(89)90038-4

[24] Bassiouny, E., Ghaleb, A. F., and Maugin, G. A., "Thermodynamical Formulation for Coupled Electromechanical Hysteresis Effects, 4: Combined Electromechanical Loading," *International Journal of Engineering Science*, Vol. 27, No. 8, 1989, pp. 989–1000.

[25] McMeeking, R. M., and Landis, C. M., "A Phenomenological Multi-Axial Constitutive Law for Switching in Polycrystalline Ferroelectric Ceramics," *International Journal of Engineering Science*, Vol. 40, No. 14, 2002, pp. 1553–1577. doi:10.1016/S0020-7225(02)00033-2

[26] Lu, X., and Hanagud, S., "Extended Thermodynamic Model for Piezoelectric Ceramics," *42nd AIAA Structures, Structural Dynamics, and Materials Conference*, AIAA, Reston, VA, 2001, pp. 1306–1316.

[27] Lemaitre, J., and Chaboche, J. L., *Mechanics of Solid Materials*, Cambridge Univ. Press, Cambridge, England, U.K., 1995.

[28] Lubliner, J., *Plasticity Theory*, MacMillan, New York, 1990.

[29] Ahmad, S. N., Upadhyay, C. S., and Venkatesan, C., "Electro-Thermo-Elastic Formulation for the Analysis of Smart Structures," *Smart Materials and Structures*, Vol. 15, No. 2, 2006, pp. 401–416. doi:10.1088/0964-1726/15/2/021

[30] Ahmad, S. N., Upadhyay, C. S., and Venkatesan, C., "Linear and Nonlinear Analysis of a Smart Beam Using General Electro-thermoelastic Formulation," *AIAA Journal*, Vol. 42, No. 4, 2004, pp. 840–849.

[31] Sateesh, V. L., Upadhyay, C. S., and Venkatesan, C., "Thermodynamic Modeling of Hysteresis Effects in Piezoceramics for Application to Smart Structures," 15th AIAA/ASME/AHS Adaptive Structures Conference, AIAA, Reston, VA, AIAA Paper 2007-1743, 2007.

[32] Kamlah, M., "Ferroelectric and Ferroelastic Piezoceramics: Modeling of Electromechanical Hysteresis Phenomena," *Continuum Mechanics and Thermodynamics*, Vol. 13, No. 4, 2001, pp. 219–268.

A. Palazotto
Associate Editor